

Jahn-Teller distortion and electronic correlation effects in undoped manganese perovskites

Patrizia Benedetti and Roland Zeyher

Max-Planck-Institut für Festkörperforschung, Heisenbergstrasse 1, 70569 Stuttgart, Germany

(July 2, 2021)

The formation of a long-range Jahn-Teller distortion in undoped manganites is studied within the dynamical mean-field theory taking both electron-phonon and electron-electron interactions into account. We find that the observed insulating behavior at temperatures above the Jahn-Teller transition and the bond-length changes below it can most naturally be explained by assuming a strong electronic repulsion and a rather weak electron-phonon coupling.

The physics of manganese oxides $\text{Re}_{1-x}\text{A}_x\text{MnO}_3$ (Re is a rare earth metal ion such as La or Pr, A a divalent alkali such as Sr or Ca) is characterized by strong electronic [1] and electron-phonon [2,3] interactions. Due to the mainly local nature of these interactions the Dynamical Mean-Field (DMF) theory [4,5] seems to be an appropriate tool for investigations of these systems. In the following we will extend previous treatments [3,6,7] by including both electron-phonon and electron-electron interactions and also by allowing for phases with long-range order. We will confine ourselves to the undoped case $x = 0$ and study, in particular, the question whether the observed Jahn-Teller distortion is driven more by the electron-phonon coupling or by electronic correlations.

Taking the limit of a very large Hund's rule coupling between the core $3/2$ spins and the e_g electrons the resulting simplified Hamiltonian reads [8]

$$H = - \sum_{ij\alpha\alpha'} t_{ij}^{\alpha\alpha'} (c_{i\alpha}^+ c_{j\alpha'} + H.c.) - \frac{U}{2} \sum_{i\gamma} T_{i\gamma} T_{i\gamma} + \frac{1}{2} \sum_{i\gamma} [(\partial_t \phi_{i\gamma})^2 + \omega_0^2 \phi_{i\gamma}^2] + g \sum_{i\gamma} \phi_{i\gamma} T_{i\gamma}, \quad (1)$$

with

$$T_{i\gamma} = \sum_{\alpha\alpha'} c_{i\alpha}^+ \sigma_{\gamma}^{\alpha\alpha'} c_{i\alpha'}. \quad (2)$$

$c_{i\alpha}^+$ ($c_{i\alpha}$) creates (destructs) an electron on the i th Mn site in the e_g orbital $\alpha = \uparrow\downarrow$, with $|\uparrow\rangle = d_{x^2-y^2}$, $|\downarrow\rangle = d_{3z^2-r^2}$. Because the Hund's rule coupling constant has assumed to be infinitely large there are no spin indices in H . The hopping elements t depend in the DMF theory on the background of the core spins. In the case of a ferromagnetic background t is given by the bare hopping element, for a paramagnetic background t contains reduction factors [3] due to the double exchange mechanism. In the following we take for simplicity $t_{ij}^{\alpha\alpha'} = \delta_{\alpha\alpha'} t_{ij}$. The pseudospin operator T is defined in Eq. (2) where the index γ always runs only over $\gamma = x, z$ where x and z denote the corresponding Pauli matrices in Eq. (2). The effective Hubbard constant U is equal to $U' - J$, where U' is the inter-orbital Coulomb and J the exchange constant of the two e_g orbitals. $\phi_{i\gamma}$ denote the two normal

Jahn-Teller modes of the six oxygens surrounding the i th Mn site and having the local e_g symmetry. ∂_t is the time derivative and ω_0 and g are the frequency and the coupling constant of the phonons.

The Hamiltonian Eq. (1) together with the condition $t_{ij}^{\alpha\alpha'} = \delta_{\alpha\alpha'} t_{ij}$, is not only invariant under the transformations of the octahedral point group but also under infinitesimal rotations in orbital space. This larger symmetry is due to the fact that H contains only invariants which are bilinear in the fields. Using the rotational symmetry we can thus omit components with $\gamma = x$ in Eq. (1) within a good approximation, yielding [7]

$$H = - \sum_{ij\alpha} t_{ij} (c_{i\alpha}^+ c_{j\alpha} + H.c.) + U \sum_i n_{i\uparrow} n_{i\downarrow} + \frac{1}{2} \sum_i [(\partial_t \phi_i)^2 + \omega_0^2 \phi_i^2] + g \sum_i (n_{i\uparrow} - n_{i\downarrow}) \phi_i, \quad (3)$$

where ϕ_i denotes the field ϕ_{iz} .

We want to investigate also the case where the orbitals order in a long-range anti-ferro orbital pattern. We therefore allow for broken symmetry and divide the lattice into two inequivalent sublattices A and B. Within the DMF theory the action associated with the Hamiltonian (1) reduces to two single impurity actions $S_{\text{eff},i}$ where $i = A, B$ and A and B stand for one site on the sublattices A and B , respectively. The two impurity actions read

$$S_{\text{eff},i} = \int_0^\beta d\tau \int_0^\beta d\tau' \sum_{\alpha=\uparrow\downarrow} c_{i\alpha}^* (\tau) G_{0i\alpha}^{-1} (\tau - \tau') c_{i\alpha} (\tau') - \frac{1}{2} \int_0^\beta d\tau \phi_i (\tau) \left(-\frac{d^2}{d\tau^2} + \omega_0^2 \right) \phi_i (\tau) - g \int_0^\beta d\tau [n_{i\uparrow} (\tau) - n_{i\downarrow} (\tau)] \phi_i (\tau) - U \int_0^\beta d\tau n_{i\uparrow} (\tau) n_{i\downarrow} (\tau). \quad (4)$$

The two local Green's functions are related by

$$G_{A\alpha} = G_{B\bar{\alpha}}, \quad (5)$$

where $\bar{\alpha}$ is the orbital different from α . The relations between the Weiss field $G_{0i\alpha}$ and the local Green's function become in the case of the Bethe lattice [4]

$$\begin{aligned} G_{0A\alpha}^{-1} &= i\omega_\nu + \mu - t^2 G_{B\alpha} \\ G_{0B\alpha}^{-1} &= i\omega_\nu + \mu - t^2 G_{A\alpha}. \end{aligned} \quad (6)$$

Decoupling the last term in Eq. (4) by means of a Hubbard-Stratonovich transformation and integrating out the electronic degrees of freedom we obtain the new impurity actions

$$\begin{aligned} S_{eff,i} = & -\frac{1}{2} \int_0^\beta d\tau \phi_i(\tau) \left(-\frac{d^2}{d\tau^2} + \omega_0^2 \right) \phi_i(\tau) \\ & - \frac{1}{2} \int_0^\beta d\tau y_i^2(\tau) + Tr \ln[G_{0i\uparrow}^{-1} - (g\phi_i + \sqrt{U}y_i)] \\ & + Tr \ln[G_{0i\downarrow}^{-1} + (g\phi_i + \sqrt{U}y_i)]. \end{aligned} \quad (7)$$

$y_i(\tau)$ denotes the Hubbard-Stratonovich (HS) field. Using Eq. (7) the local Green's functions have the exact representations

$$G_{i\alpha}(\tau - \tau') = \int D\phi_i(\tau) Dy_i(\tau) [G_{0i\alpha}^{-1}(\tau_1 - \tau_2) - \sigma_z^{\alpha\alpha}(g\phi_i(\tau_1) + \sqrt{U}y_i(\tau_1))\delta(\tau_1 - \tau_2)]_{\tau - \tau'}^{-1} e^{S_{eff,i}} / Z_i, \quad (8)$$

for $i = A, B$. Z_i is the partition function. Eqs. (5)-(8) represent a closed system of equations for the Green's functions of the two coupled sublattices.

From the equation of motion for the field ϕ_i one obtains

$$\begin{aligned} \langle \phi_i \rangle &= -\frac{g}{\omega_0^2} (\langle n_{i\uparrow} \rangle - \langle n_{i\downarrow} \rangle), \\ \langle \phi_A \rangle &= -\langle \phi_B \rangle. \end{aligned} \quad (9)$$

Here $\langle n_{i\alpha} \rangle$ is the average number of electrons in the orbital α on the sublattices $i = A, B$. The quantity $\langle n_{i\uparrow} \rangle - \langle n_{i\downarrow} \rangle$ can be considered as a staggered order parameter. $\langle \phi_i \rangle$ is the expectation value of the phonon field ϕ_i . Moreover, the average number of electrons per manganese site is one in the undoped case, so that $n_i = \langle n_{i\uparrow} + n_{i\downarrow} \rangle = 1$.

Assuming that the two fields ϕ and y vary only slowly in time $S_{eff,i}$ can be calculated by means of a gradient expansion [9]. The leading contribution to $S_{eff,i}$ is local in time and is given by the following effective potential

$$\begin{aligned} V_i(\phi(\tau), y(\tau)) = & \frac{\omega_0^2}{2} \phi_i^2(\tau) + \frac{1}{2} y_i^2(\tau) \\ & - T \sum_\nu e^{i\nu 0^+} \ln[1 - (g\phi_i(\tau) + \sqrt{U}y_i(\tau))G_{0i\uparrow}(i\nu)] \\ & - T \sum_\nu e^{i\nu 0^+} \ln[1 + (g\phi_i(\tau) + \sqrt{U}y_i(\tau))G_{0i\downarrow}(i\nu)]. \end{aligned} \quad (10)$$

The lowest-order non-local contributions to $S_{eff,i}$ are functionals of ϕ_i and y_i which include also at least one time derivative $\partial\phi_i/\partial\tau$ or $\partial y_i/\partial\tau$.

For the evaluation of G in Eq. (8) we distinguish between several cases. First we consider the case $U = 0$ where the model reduces to a pure Jahn-Teller system and the collective coordinate y drops out. Starting from an educated guess for $G_{0i\alpha}$ we calculate first the effective potentials V_i using Eq. (10) and transforming the sums over Matsubara frequencies into integrals along the real axis. $G_{i\alpha}$, as given by Eq. (8), is calculated by using expansions around the extremal paths of $S_{eff,i}$. In general, there are two time-independent paths $\bar{\phi}_r, r = 1, 2$, corresponding to the two minima of V_i , and one time-dependent instanton path. The contribution from the latter is very small for our considered temperatures and atomic masses [9] so we will neglect it together with the non-local part of $S_{eff,i}$. Around each minimum $\bar{\phi}_r$ we generate a Migdal-Eliashberg-like expansion. It is governed by the Migdal parameter ω_0/t which is rather small in the manganites. Detailed calculations show [9] that for all finite coupling strengths it is sufficient to include only the Hartree and the Fock terms. First-order vertex corrections to these terms turn out to be smaller by a factor $\lambda\omega_0/t$, λ being the electron-phonon coupling constant defined by $\lambda = g^2/\omega_0^2 t$. In calculating the Fock term we use a phonon propagator which has been constructed from the exact eigenvalues and eigenfunctions of the Schrödinger equation describing an atom in the effective potential V_i . In this way anharmonic effects are fully taken into account. From Eq. (6) we obtain new Weiss fields $G_{0i\alpha}$ as input for another cycle. The procedure is repeated until self-consistency is reached. From now on all energies are expressed in units of the hopping matrix element t , unless differently specified.

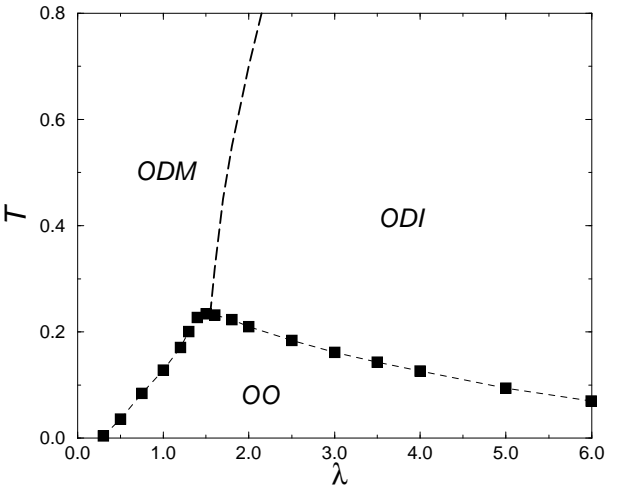


FIG. 1. T - λ phase diagram for electrons coupled only to Jahn-Teller phonons. OO: ordered orbital phase; ODM and ODI: metallic and insulating disordered orbital phases, respectively.

Numerical results are shown in Fig. 1 where the critical temperatures are plotted versus the electron-phonon coupling λ . The phonon frequency has been fixed to $\omega_0 = 0.04$. Three phases can be identified: 1) an insulating phase in which the orbitals are ordered (OO), 2) a phase in which the orbitals are disordered and the system is metallic (ODM), 3) a phase in which the orbitals are disordered and the system is insulating (ODI). The thick dashed line shows the metal-insulator transition temperature, the squares indicate the calculated points where the orbital order-disorder transition takes place. This is a second-order phase transition where the order parameters $\langle \phi_i \rangle$ go continuously to zero as the temperature approaches T_c from below.

In the orbital disordered phase the two e_g orbitals are degenerate and occupied with the same probability. The effective potentials V_i are symmetric with respect to $\phi_i = 0$ and two regimes can be distinguished. In the strong coupling regime, $\lambda > \lambda_c(T)$, the potential shows two deep and well separated minima leading to a gap in the density of electronic states. In this case the system is in the insulating phase ODI. In the weak coupling regime, $\lambda < \lambda_c(T)$, the potential has only one minimum and the system is in the metallic phase ODM. In the ordered phase the effective potential of each sublattice is asymmetric with respect to $\phi_i = 0$. In the weak coupling regime there is only one minimum and it is shifted with respect to the origin by an amount $\Delta\phi_i \sim \langle \phi_i \rangle$. In contrast to that in the strong coupling case such a shift is also accompanied by a lowering of one minimum with respect to the other minimum. The interaction with the phonons lifts the orbital degeneracy in an opposite way on the two sublattices. This creates a disproportion in the occupation probability of the two orbitals leading to the formation of a staggered pattern of occupied orbitals and consequently to the experimentally observed cooperative distortion of the oxygen bonds. A qualitatively similar phase diagram has recently been given in Ref. [10] for the Holstein model with infinitely heavy atoms.

Experimentally the static Jahn-Teller distortion in PrMnO_3 occurs around $T_c \sim 850\text{K}$ [11] and in LaMnO_3 around $T_c \sim 750\text{K}$. Above T_c these systems are insulators. If we compare these data with our phase diagram in Fig. 1 we obtain, taking $t = 0.7\text{eV}$ [13], a value for λ of about 5 in the insulating region. This is an extremely large value. In the following we show that a more realistic picture is obtained if one also includes the Coulomb repulsion between the e_g electrons.

$S_{eff,i}$ depends on the two fields ϕ_i and y_i if also the electron-electron interaction is included. A reduction to one field is in this case possible if one treats the phonon field in the static approximation. The physical basis for this is the inequality $\omega_0 \ll t$, which says that the effective phonon mass is much larger than the electronic one. Performing then the following change of variables in Matsubara space

$$y_i(i\omega_n)\sqrt{U} + g\phi_i(0)\delta_{n,0} = x_i(i\omega_n)\sqrt{U+\lambda}, \quad (11)$$

we can integrate out the $\phi_i(0)$ coordinate and obtain the effective action

$$\begin{aligned} S_{eff,i} = & -\frac{1}{2} \sum_n \left(1 + \frac{\lambda}{U} - \frac{\lambda}{U} \delta_{n,0} \right) x_i(i\omega_n) x_i(-i\omega_n) \\ & + \text{Tr} \ln[G_{0i\uparrow}^{-1} - \sqrt{U+\lambda} x_i] \\ & + \text{Tr} \ln[G_{0i\downarrow}^{-1} + \sqrt{U+\lambda} x_i]. \end{aligned} \quad (12)$$

The limit $\lambda \rightarrow 0$ correctly reproduces the action for the Hubbard model and the limit $U \rightarrow 0$ the action for the static Jahn-Teller system. In the following we will concentrate on the case $U \gg \lambda$. Using the local approximation for the $\text{Tr} \ln$ term the effective potential reads

$$\begin{aligned} V_i(x_i(\tau)) = & \frac{1}{2} x_i(\tau)^2 \\ & - T \sum_{\nu} e^{i\nu 0^+} \ln[1 - \sqrt{U+\lambda} x_i(\tau) G_{0i\uparrow}(i\nu)] \\ & - T \sum_{\nu} e^{i\nu 0^+} \ln[1 + \sqrt{U+\lambda} x_i(\tau) G_{0i\downarrow}(i\nu)]. \end{aligned} \quad (13)$$

This means that there is no kinetic term in Eq. (12). $G_{i\alpha}$ can again be calculated by using expansions around the potential minima $\bar{\phi}_r$. The propagator for the field x becomes instantaneous and thus can be put to zero. As a result only the Hartree term in each expansion around $\bar{\phi}_r$ contributes. The lowest-order corrections to the field propagator would come from the non-local part in $S_{eff,i}$ and lead to a relaxational dynamics for the field x . Since for all couplings the damping is substantially smaller than ω_0 these corrections are, however, small [9].

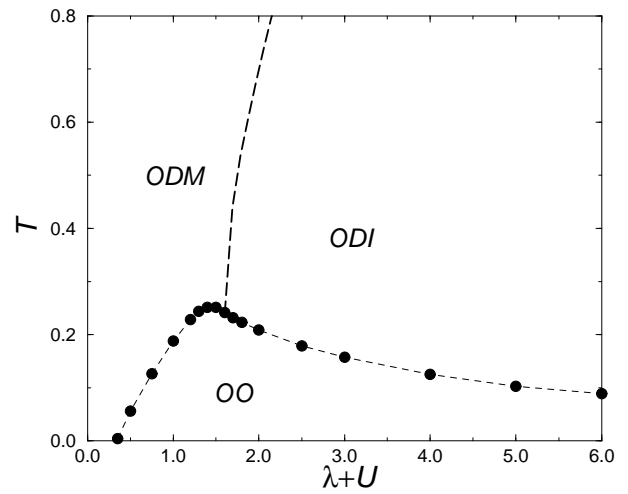


FIG. 2. Phase diagram showing the critical temperature versus $\lambda + U$ for a static phonon and dynamic HS field assuming $U \gg \lambda$.

We have solved Eqs.(11)-(13) in a self-consistent way. Figure 2 shows the calculated phase diagram for the case where the phonon, but not the Hubbard-Stratonovich field, is treated in the static approximation. We also assumed $U \gg \lambda$ which allows to lump the two coupling constants together into an effective coupling constant $\lambda + U$. The black dots are the calculated critical temperatures as a function of $\lambda + U$. Our previous discussion of the three phases OO, ODM, and ODI in Fig. 1 also applies more or less to Fig. 2. Remarkable is the close similarity of the phase boundaries in Figs. 1 and 2, even on a quantitative level. Let us estimate the Jahn-Teller coupling in the present case. Using $t = 0.7\text{eV}$, $T_c \sim 0.1\text{t}$ and the fact that LaMnO_3 is insulating above T_c we obtain from Fig. 2 an effective coupling $\lambda + U \sim 5.3$ and $\Delta n = n_{A\uparrow} - n_{A\downarrow} \sim 1$. The energy associated with the Jahn-Teller distortion can be estimated from the experimental data and is about $E \sim 0.14\text{eV}$. From that, making use of Eq. (9) with $\Delta n \sim 1$, we obtain $\lambda \sim 0.3$. This means that the experimental data can easily be reproduced with $U \sim 3.5\text{eV}$ and $\lambda \sim 0.3$. An independent determination of U yielded 3.8eV [14] and is thus in good agreement with our value. The value $\lambda = 0.3$ associated with one branch of phonons is on the one hand side not small indicating the importance of phonons. On the other hand, the critical coupling strength for a metal-insulator transition is according to Fig. 1 about 1.5 and thus five times larger than the obtained value. This means that the insulating phase above T_c as well as the Jahn-Teller transition itself in PrMnO_3 and LaMnO_3 are mainly caused by electronic correlations and not by the electron-phonon coupling.

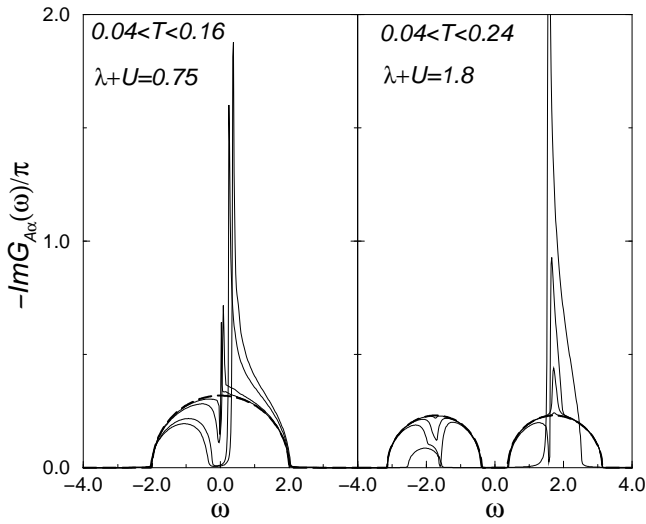


FIG. 3. Temperature dependence of the electronic density of states on the sublattice A for the orbital $\alpha = \uparrow$ versus frequency. The left and right panels correspond to the weak- and strong-coupling cases, respectively.

Fig. 3 shows the evolution of the electronic density of states (DOS) of one e_g orbital on the sublattice A with temperature for two different values of the effective coupling constant $\lambda + U$. The solid lines cover the temperature range from far below the orbital ordering temperature T_c to just below T_c . The dashed line shows the DOS just above T_c . The left panel presents data in the weak-coupling regime $\lambda + U = 0.75$. Below the critical temperature the DOS shows an asymmetry with respect to the Fermi level $\omega = 0$, signaling a disproportion of the average electronic occupation of each e_g orbital. As a result, $n_{A\uparrow} \neq n_{A\downarrow}$ and, at the same time, $n_{A\uparrow} = n_{B\downarrow}$ holds. The difference between $n_{A\uparrow}$ and $n_{A\downarrow}$ increases with decreasing temperature. At low enough temperature a gap opens in the DOS at $\omega = \text{Re } G_{B\alpha}(\omega) + \sqrt{\lambda + U} \langle x_A \rangle$. $\text{Re } G_{B\alpha}(\omega)$ denotes the real part of $G_{B\alpha}(\omega)$ and $\langle x_A \rangle$ the expectation value of the field x for the action Eq. (12) on the sublattice A. Above T_c the system is metallic. The right panel in Fig. 3 shows data for $\lambda + U = 1.8$. Above T_c the system is in the strong-coupling regime where the effective potential has two well separated minima causing two symmetric subbands in the DOS. With decreasing temperature spectral weight is transferred from the lower to the upper band leading to an asymmetry in the spectra. The gap stays practically constant until, at low enough temperatures, the orbital ordering gap becomes larger than the charge gap and almost all spectral weight is transferred to the right band. At $T=0.04t$ we have $\Delta n = n_{A\uparrow} - n_{A\downarrow} \sim 0.86$.

As mentioned previously our Hamiltonian Eq. (1) is for the case of isotropic hopping matrix elements invariant under continuous rotations in orbital space which can be characterized by an angle θ [8]. As a result θ is not determined by Eq. (1) but by residual interactions such as anisotropic hoppings, higher-order invariants in the couplings due, for instance, to a quadratic electron-phonon coupling. The real situation in the manganites is even more complicated because of the observed tilt of the oxygen octahedra and the important role played by the oxygen degrees of freedom. However, we can discuss with our Hamiltonian the temperature dependence of the electron density on the Mn sites if we choose, for instance, $\theta = \pi/4$ which is not far away from the experimental situation in PrMnO_3 and LaMnO_3 . Fig. 4 shows for $\lambda + U = 4.0$ the angular dependence of the electronic density on the two sublattices $i = A, B$, defined by

$$\rho_i(\theta, \varphi) = n_{i\uparrow} |\langle \uparrow | \theta, \varphi \rangle|^2 + n_{i\downarrow} |\langle \downarrow | \theta, \varphi \rangle|^2, \quad (14)$$

$\langle \uparrow | \theta, \varphi \rangle$ and $\langle \downarrow | \theta, \varphi \rangle$ denote the angular components of $|\uparrow\rangle = (d_{x^2-y^2} + d_{3z^2-r^2})/\sqrt{2}$ and $|\downarrow\rangle = (d_{x^2-y^2} - d_{3z^2-r^2})/\sqrt{2}$, respectively.

$$- \frac{1}{2} \int_0^\beta d\tau y_i^2(\tau). \quad (15)$$

Changing variables as

$$\sqrt{U}x_i(\tau) = \sqrt{U}y_i(\tau) - g\phi_i(\tau), \quad (16)$$

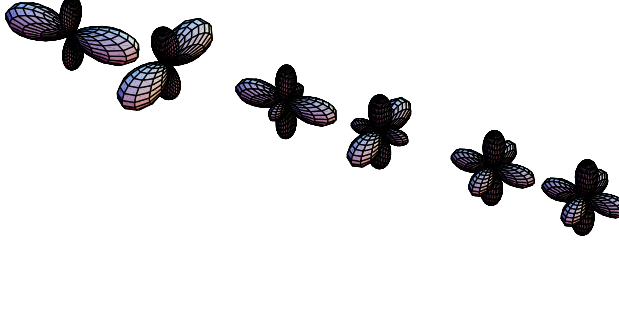


FIG. 4. Angular dependence of the electronic density on two adjacent Mn sites for three different temperatures and $\lambda + U = 4.0$. The vertical lobe points into the c -direction, the horizontal ones alternatively into the a - and b -directions.

The first pair of densities on the left in Fig. 4 corresponds to the temperature $T = 0.04t < T_c$ and the site occupancies $n_{A\uparrow} = 0.98$ and $n_{B\uparrow} = 1 - n_{A\uparrow} = 0.02$. The electronic charge distribution is strongly anisotropic leading to alternating short and long Mn-O bonds along the a - and b - directions on the two sublattices. The bond in the c -direction remains constant. The pair of densities in the middle of Fig. 4 corresponds to $T = 0.116t < T_c$ and the site occupancy $n_{A\uparrow} = 0.67$. One recognizes that the increasing temperature decreases the anisotropy of the electronic distribution and thus also the distortion of the octahedra. Finally, the pair of densities at the right depicts the electron distribution on the two sublattices for $T = 0.16t > T_c$ and $n_{A\uparrow} = n_{B\uparrow} = 0.5$. The electrons are now uniformly distributed along the three axes and the oxygens occupy the equilibrium positions of the cubic perovskite lattice.

The above calculations for the case involving both the electron-electron and the electron-phonon interaction were based on classical, infinitely heavy atoms and the condition $U \gg \lambda$. Here we want to point out that there is another tractable case, that is when the fluctuations for the combined system are treated in a Gaussian approximation. Performing a Hubbard-Stratonovich transformation in Eq. (4) we obtain

$$\begin{aligned} S_{eff,i} = & \int_0^\beta d\tau \int_0^\beta d\tau' \sum_{\alpha=\uparrow\downarrow} c_{i\alpha}^*(\tau) G_{0i\alpha}^{-1}(\tau - \tau') c_{i\alpha}(\tau') \\ & - \frac{1}{2} \int_0^\beta d\tau \phi_i(\tau) \left(-\frac{d^2}{d\tau^2} + \omega_0^2 \right) \phi_i(\tau) \\ & - \int_0^\beta d\tau [\sqrt{U}y_i(\tau) - g\phi_i(\tau)][n_{i\uparrow}(\tau) - n_{i\downarrow}(\tau)] \end{aligned}$$

and performing the Gaussian integral over the phonon field we obtain [7]

$$\begin{aligned} S_{eff,i} = & \int_0^\beta d\tau \int_0^\beta d\tau' \sum_{\alpha=\uparrow\downarrow} c_{i\alpha}^*(\tau) G_{0i\alpha}^{-1}(\tau - \tau') c_{i\alpha}(\tau') \\ & - \int_0^\beta d\tau \sqrt{U}x_i(\tau)[n_{i\uparrow}(\tau) - n_{i\downarrow}(\tau)] \\ & - \frac{1}{2} \sum_n \left(\frac{\omega_n^2 + \omega_0^2}{\omega_n^2 + \Omega_0^2} \right) x_i(-\omega_n)x_i(\omega_n), \end{aligned} \quad (17)$$

where $\Omega_0 = \omega_0\sqrt{1 + \lambda/U}$ is the renormalized phonon frequency. We now integrate out the electronic degrees of freedom. The effective action depends only on x_i and it reads

$$\begin{aligned} S_{x,i} = & -\frac{1}{2} \sum_n \left(\frac{\omega_n^2 + \omega_0^2}{\omega_n^2 + \Omega_0^2} \right) x_i(-\omega_n)x_i(\omega_n) \\ & + Tr \log[G_{0s\uparrow}^{-1} - \sqrt{U}x_i] + Tr \log[G_{0s\downarrow}^{-1} + \sqrt{U}x_i]. \end{aligned} \quad (18)$$

Expanding up to the first order in ω_n^2 we obtain

$$\begin{aligned} S_{x,i} = & -\frac{1}{2} \int_0^\beta d\tau x_i(\tau) \left[-\frac{1}{\omega_0^2(1+U/\lambda)} \frac{d^2}{d\tau^2} + 1 \right] x_i(\tau) \\ & + Tr \log[G_{0s\uparrow}^{-1} - \sqrt{U+\lambda}x_i] \\ & + Tr \log[G_{0s\downarrow}^{-1} + \sqrt{U+\lambda}x_i]. \end{aligned} \quad (19)$$

The action Eq. (19) is no longer a function of only the sum $U + \lambda$ but depends on both variables U and λ in an independent way.

The approximate action Eq. (19) reproduces correctly the cases without phonons ($\lambda = 0$) and without electronic correlations ($U = 0$). Moreover, for $T \gg \omega_0\sqrt{1+U/\lambda}/2\pi$ only the zero-frequency variable $x_i(0)$ contributes to the action corresponding to the case where x_i can be treated as a classical and time-independent variable. Keeping all terms in Eq. (19) is equivalent to an Gaussian approximation for temporal fluctuations. Eq. (19) therefore represents an interpolation between the two exactly treated cases $\lambda = 0$ and $U = 0$ which is valid if the temperature is not much smaller than the renormalized frequency $\omega_0\sqrt{1+U/\lambda}/2\pi$. The action given by Eq. (19) can be treated with the same methods as described above for the phonon-only case. Figure 5 shows the resulting phase diagram for a fixed $\lambda = \lambda_0 = 0.3$ and $\omega_0 = 0.04$. We have chosen $\lambda_0 = 0.3$ as a representative value for the electron-phonon coupling, according to what we have estimated above. Comparison of Figs. 2 and 5 indicates that treating the atoms

quantum-mechanically and not classically with infinite heavy masses yields only small changes justifying the above simpler treatment based on Eqs. (11)-(13).

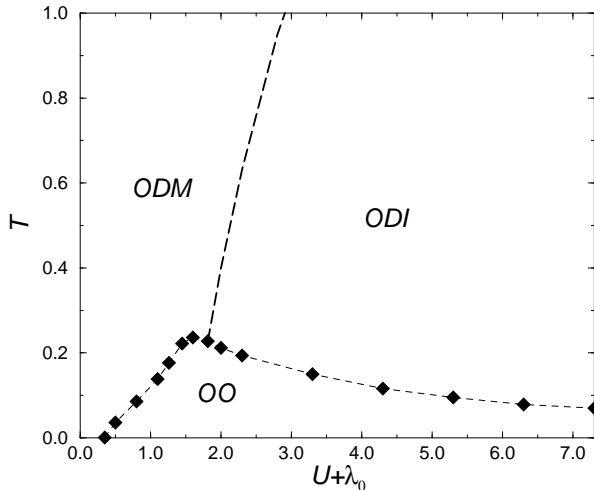


FIG. 5. Phase diagram showing the critical temperature versus $U + \lambda_0$, with $\lambda_0 = 0.3$, for dynamic phonons and HS fields in a Gaussian approximation.

In conclusion, we have extended previous treatments of manganites within the DMF theory including also phases with long-range order and, in addition to the electron-phonon coupling, the electron-electron interaction. Using expansions around stationary paths of the action which are controlled by the Migdal parameter we were able to treat the weak- and the strong-coupling cases on an equal footing. However, since the temporal fluctuations of the phonon and the Hubbard-Stratonovich (HS) fields are different we considered three special cases: a) the phonon-only case; b) the case where the phonons are treated statically, the HS field dynamically; and c) treating both fields dynamically in the Gaussian approximation. For each case the phase diagram was shown. Applying the results to undoped manganites it was concluded that the observed Jahn-Teller transition is mainly driven by the electron-electron and only to a lesser extent by the electron-phonon interaction. Our simple model for the

Jahn-Teller transition in manganites could be made more realistic by including additional interactions. Anisotropic hopping terms, an electron-phonon interaction of second order, and the explicit treatment of oxygen degrees of freedom would remove the invariance of our Hamiltonian with respect to infinitesimal rotations in orbital space and thus determine the electronic density uniquely. Furthermore, instead of one effective electron-electron interaction constant, distinct inter- and intra- orbital interaction terms should be considered, which would allow to include also low-spin states.

Acknowledgment: The authors thank A. M. Oleś for a careful reading of the manuscript and for discussions. P.B. acknowledges fruitful discussions with J. van den Brink.

- [1] C.M. Varma, Phys. Rev. B **54**, 7328 (1996).
- [2] I. Solovyev, N. Hamada, and K. Terakura, Phys. Rev. Lett. **76**, 4825 (1996).
- [3] A.J. Millis, B.I. Shraiman, and R. Mueller, Phys. Rev. Lett. **77**, 175 (1996).
- [4] A. Georges, G. Kotliar, W. Krauth and M.J. Rozenberg Rev. Mod. Phys. **68**, 13 (1996).
- [5] W. Metzner and D. Vollhardt, Phys. Rev. Lett. **62**, 324 (1989).
- [6] A.J. Millis et al., Phys. Rev. B **54**, 5389 and 5405 (1996).
- [7] N. Nagaosa, S. Murakami, and H.C. Lee, Phys. Rev. B **57**, R6767 (1998).
- [8] R. Maezono, S. Ishihara, and N. Nagaosa, cond-mat/9805267.
- [9] P. Benedetti and R. Zeyher, Phys. Rev. B **56**, in press (1998), cond-mat/9807094.
- [10] S. Ciuchi and F. de Pasquale, preprint.
- [11] Z. Jirák et al., J. Magn. Magn. Mat. Materials **53**, 153 (1985).
- [12] J. Rodríguez-Carvajal et al., Phys. Rev. B **57**, R3189 (1998).
- [13] T. Saitoh et al., Phys. Rev. B **51**, 13942 (1995).
- [14] L.F. Feiner and A.M. Oleś, Phys. Rev. B **56**, in press (1998), cond-mat/9805011.